Mechanistic subtleties in the cyclopentannelation of allenolate allyl carbamates: the origin of the center-to-center chirality transfer†

Olalla Nieto Faza, Carlos Silva López, Rosana Álvarez and Ángel R. de Lera*

Received (in Cambridge, UK) 12th May 2005, Accepted 27th June 2005
First published as an Advance Article on the web 27th July 2005
DOI: 10.1039/b506601h

The stereospecific rearrangement of allene carbamates i to alkylidenecyclopentenones iii is concerted, displays charge donation from the $\pi^*_{allenonate}$ to the $\sigma^*_{C\text{-leaving group}}$, and shows mechanistic features of both pericyclic and ionic processes, modulated in part by the degree of ionic interaction ($O^-\ldots Li^+$) in the putative intermediate allenolate ii.

Following transfer of the *N*,*N*-diisopropylcarbamoyl group on C_4 to the alkoxide at C_3, chiral non-racemic allenyl carbamates **i-a** and **i-b** afford alkylidenecyclopentenones **Z-iii** and **E-iii**, respectively, by stereospecific ring closure (Scheme 1).[1] (a*R*,*S*)-**i-a** yields exclusively (*Z*,*S*)-**Z-iii**, and (a*R*,*R*)-**i-b** affords (*E*,*R*)-**E-iii**, in a process displaying complete center-to-center chirality transfer. The reaction was considered as a "hybrid of an intramolecular vinylic cycloalkylation of a lithium allenolate and a modified Nazarov cyclization".

Previous insight into the nature of electrocyclic processes of charged species,[2] such as the hydroxypentadienyl cation electrocyclization, fueled our interest in the mechanism of reaction **i** → **iii** and prompted this theoretical study. For a complete center-to-center chirality transfer to occur, the dissociation of the *N*,*N*-diisopropylcarbamoyloxy group of **ii** must not precede the cyclization as, if this were the case, the C_1–C_5 bond forming step would formally be a four-electron pentadienyl cation electrocyclization (a Nazarov-type system), and thus produce an alkylidenecyclopentenone with the less congested *Z* geometry,[1,3] regardless of the configuration at C_3 of **i**. Since we could not locate transition structures corresponding to a concerted cyclization accompanying an incipient carbamoyl transfer from C_4 to C_3 either, the proposed intermediate **ii** was considered to be the likeliest species experiencing the ring-closure reaction. Simplified models (structures **1**) of allenolate **ii** were then selected (Scheme 2) to investigate the mechanism behind this unexpected preference for a sterically penalized path. The *N*,*N*-diisopropylcarbamoyl group was replaced with a simpler acetate in systems with methyl groups at C_1 and C_6. Bulkier phenyl and *t*-Bu at the same positions (as in **i**) were also surveyed to gauge steric effects on stereoselectivity. The uncertainty of the extent of lithium coordination after the carbamoyl transfer step that leads to **ii** made us select as reactants both the naked and the lithium allenolate, the actual behaviour in solution being expected to lie somewhere between these two extreme descriptions.

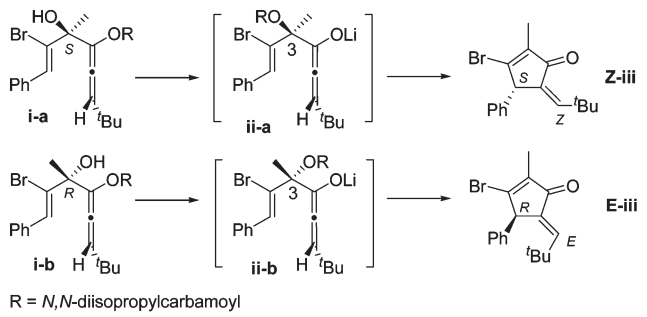

Scheme 1 1. *n*-BuLi, TMEDA, toluene, 1 h, −78 °C, 1 h, rt; 2. 2 N HCl.

Transition states labeled **tsE** and **tsZ** were located for each diastereomer of **1**. In both cases, the observed trends fully agree with the experimental findings: the configuration of the product is completely controlled by that of C_3 in the reactant. The differences in activation energies for the two competing paths range from 2.76 to 5.06 kcal mol^{-1}, ensuring complete selectivity: cyclization of **1a** results in (*S*,*Z*)-**2** *via* **tsZ**, while **1b** yields (*R*,*E*)-**2** through **tsE** (see Table 1). The only noticeable effect in the ring closure of system **1** with bulky Ph and *t*-Bu groups on C_1 and C_6 is the reduction of $\Delta\Delta G^{\ddagger}$ when the favored path is the most hindered **tsE** from **1b**, which confirms that the observed stereoselection is not of steric origin.

Having discarded both a pentadienyl cation cyclization and a cyclization at the tetrahedral cyclic trans-carbamoylation stage intermediate, two mechanisms that start from allenolate **ii** appear to be feasible: a stepwise process, with the vinylic cycloalkylation preceding the carbamoyloxy departure, and a concerted one. In the latter case, both an ionic and a pericyclic mechanism could reasonably be postulated. Further inspection of Table 1 can help to shed light on the nature of the reaction mechanisms.

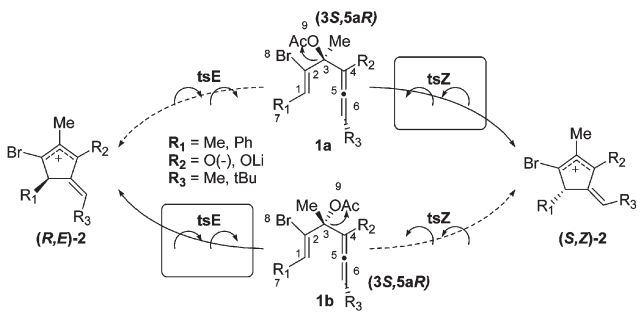

Scheme 2 Two "conrotatory" paths are described: **tsZ**, which leads to the *Z* product, and **tsE**, which results in the *E* alkylidenecyclopentenyl cation. Atom numbering used in the discussion is shown on the reactant.

Dpto. de Química Orgánica, Universidade de Vigo, Lagoas-Marcosende, 36310, Vigo, Spain. E-mail: qolera@uvigo.es; Fax: 34 986811940; Tel: 34 986812316

† Electronic supplementary information (ESI) available: computational details. See http://dx.doi.org/10.1039/b506601h

Table 1 Relative energies, $\Delta\Delta G^{\ddagger}$ ($\Delta G^{\ddagger}_{\text{fav. path}} - \Delta G^{\ddagger}_{\text{non-fav. path}}$), key geometric parameters and APT charges at C_2 (q_{C2}), for the structures discussed in the text. The charge difference between the reacting termini is also shown as q_{1-5} (q_{C1}–q_{C5}). The thermodynamic quantities are expressed in kcal mol^{-1}, the distances C_1–C_5 (d_{1-5}) and C_3–O_9 (d_{1-9}) are noted in Ångstroms, and the dihedral angle θ_{8234} in degrees. Calculations were carried out as described in ref. 10

R_2	C_3	Str.	$\Delta G^{\ddagger}$	$\Delta\Delta G^{\ddagger}$	d_{1-5}	d_{3-9}	θ_{8234}	q_{C2}	q_{1-5}
R_1 = Me, R_3 = Me									
O(−)	*R*	min	0.00		3.23	1.46			
		tsZ	15.29		2.19	1.45	86.7	−0.27	0.96
		tsZ.int	−8.96		1.53	1.45	68.0	−0.13	
		tsE	**12.12**	**3.17**	**2.19**	**1.53**	**103.8**	**−0.23**	**0.90**
OLi	*R*	min	0.00		3.15	1.51			
		tsZ	39.16		1.99	1.44	106.4	−0.01	0.05
		tsZ.int	14.91		1.54	1.48	76.5	−0.39	
		tsE	**34.00**	**5.06**	**2.06**	**1.48**	**99.2**	**−0.09**	**0.14**
O(−)	*S*	min	0.00		3.69	1.46			
		tsZ	**17.30**	**2.76**	**2.20**	**1.54**	**113.2**	**−0.15**	**0.81**
		tsE	20.06		2.20	1.45	81.7	−0.30	0.99
OLi	*S*	min	0.00		3.17	1.51			
		tsZ	**34.34**	**4.13**	**2.05**	**1.49**	**104.8**	**−0.06**	**0.08**
		tsE	38.48		1.99	1.44	99.5	−0.09	0.13
R_1 = Ph, R_3 = *t*-Bu									
O(−)	*R*	tsZ	0.00		2.12	1.45	88.0	−0.35	0.87
		tsE	**−3.23**	**3.23**	**2.17**	**1.56**	**119.1**	**−0.14**	**0.74**
	S	**tsZ**	**0.00**	**4.69**	**2.13**	**1.53**	**100.2**	**−0.29**	**0.74**
		tsE	4.69		2.13	1.44	85.9	−0.33	0.95

The C_1–C_5 and the C_3–O_9 bond distances are always equal or larger for the transition structure lower in energy, but their variation is not the same in all the series. For the naked allenolates $R_2 = O^-$, an earlier concerted transition state for the favored path is found, where the leaving group has just started to dissociate. The slightly shorter d_{1-5} distance for the alternate disfavored path reveals in turn a later transition state. Interestingly, d_{3-9} is surprisingly short (even shorter than its equivalent in the reactant) which suggests a stepwise mechanism. The same reasoning applies to the structures where the allenolate has an explicit lithium counterion, the only differences being the somewhat shorter C_1–C_5 bond distances (presumably due to the more significant charge on the naked allenolate), and the C_3–O_9 bond length, which is shorter than that of the minimum for **tsZ** and **tsE**, even if it is longer for the favored path. The Br–C_2–C_3–C_4 dihedral (θ_{8234}), together with the charges at C_2, supports this picture of low-energy concerted paths *vs.* high-energy stepwise mechanisms: the preferred paths are (with exceptions) characterized by more planar θ dihedrals, while the alternatives display pyramidalized C_2 atoms with more anionic character.

The charge difference between the cyclizing termini (q_{C1}–q_{C5}) in the transition structure is smaller for the favored paths. This could be interpreted as the result of a higher "electrocyclic" contribution to the mechanism, but is fully compatible with either an ionic or a polarized pericyclic process. Finally, IRC calculations for these transition structures,[4] and the finding of alkylidenecyclopentanone anion minima on the non-favored paths (**tsZ.int** in Table 1), confirm that these non-observed rotations are stepwise, whereas the reaction mechanism leading to products **2** is concerted, albeit rather asynchronous.

Second order perturbation theory on the framework of an NBO analysis of the wavefunction (Table 2) confirms that the transition structures lower in energy show charge donation from the allenolate ($\pi^*_{(C4-O^-)}$ or $\pi^*_{(C4-C5)}$ bonds) to the $\sigma^*_{(C3-O9)}$ bond,

Table 2 Second order perturbation energies of the interactions between NBO orbitals (kcal mol^{-1})

Structure	Interaction	tsZ	tsE
1b R_2 = O^-	$\pi^*(C_4-R_2)$–$\sigma^*(C_3-O_9)$	1.20	10.36
1a R_2 = O^-	$\pi^*(C_4-R_2)$–$\sigma^*(C_3-O_9)$	12.10	< 0.50
1b R_2 = OLi	$\pi^*(C_4-C_5)$–$\sigma^*(C_3-O_9)$	2.04	11.99
1a R_2 = OLi	$\pi^*(C_4-C_5)$–$\sigma^*(C_3-O_9)$	12.15	1.66

that is much smaller in the alternate paths. Thus, the preferred rotation is the one that allows the π-system with better donor properties (the allenolate in this case) to delocalize charge on the $\sigma^*_{(C3-O9)}$ orbital. As this donation to an antibonding orbital weakens the C_3–O_9 bond, it is expected that, when existent, it will lower the activation energy and propitiate concerted processes. This effect would be akin to the known DePuy effect on the electrocyclic ring opening of halocyclopropanes, in which the direction of disrotatory motion and hence the stereochemical outcome is the result of charge donation from the dissociating C–C bond to the antibonding orbital of the breaking C–leaving group bond (Woodward–Hoffmann–DePuy rule).[5]

An ambiguity remains in the description of the favored ring closure, since a five atom anionic cyclization, where an internal enolate attacks an alkene in an S_N2' process is indistinguishable from a process in which the leaving-group cleavage is concerted with the electrocyclization of the incipient pentadienyl cation. In the latter case, the carbamoyloxy group on C_3 must be dissociated enough in the transition structure to provide the main chain with the carbenium character needed for a cyclic conjugation of the π system. The remarkable chirality transfer observed would then reflect the preference for one of the two symmetry-allowed conrotatory modes in this formal $4\pi e^-$-electrocyclic reaction. Torquoselectivity in this case has the uncommon attribute of being induced by a substituent on the β carbon instead of the usual *ipso* induction.[6] On the other hand, the concerted ionic mechanism or intramolecular S_N2' reaction would display a preferred *anti* stereochemical outcome. No transition structures could be located for the alternative "disrotatory" reaction paths (which would yield (*R*,*Z*)-**2** and (*S*,*E*)-**2**), presumably due to either the Woodward–Hoffmann rules or to the restraints imposed by the cyclic structure, which prevent the system from adopting a Bürgi–Dunitz trajectory.

To distinguish between alternate pericyclic and ionic mechanisms with the same stereochemical outcome, geometrical features, charge distribution and orbital depiction, we turned to the analysis of the aromaticity of the transition structures. Following Zimmerman's model, the cyclic loop of orbitals in transition states of pericyclic reactions should display aromatic features. Two computational methods to characterize aromaticity were selected: the nucleus independent chemical shift (NICS) (Fig. 1) and the anisotropy of the current induced density (ACID)[8] (Fig. 2). Thus, for an aromatic transition state, a circular current would be expected, together with high values of the isotropic shielding (high negative NICS values) in the region near the cyclizing plane, a property not found in an ionic reaction.

In Fig. 1, the values obtained for **1b** with R_2 = OLi, agree with a pericyclic mechanism with an aromatic transition structure. Values for the naked enolate **1b** with $R_2 = O^-$ are however not negligible. In order to discard its aromatic nature, the vinylic cycloalkylation

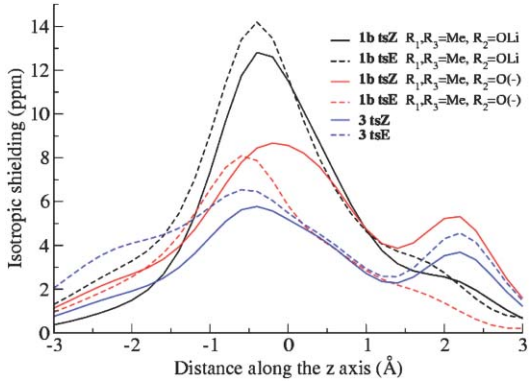

Fig. 1 Isotropic shielding *vs.* distance along the *z* axis for the studied transition structures.

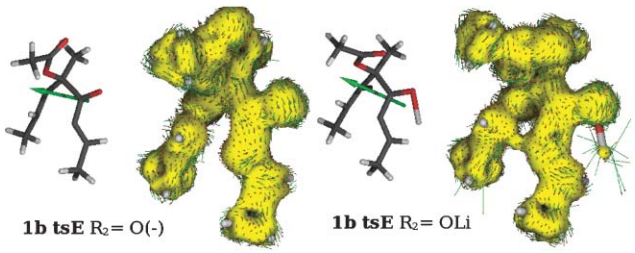

Fig. 2 ACID representation for **1b tsE** when $R_2 = O^-$ and $R_2 = OLi$. The 0.030 isodensity surface was chosen to show the cyclic induced density in the lithium allenolate, absent in the naked one.

of an analog with no leaving group at C3 (Scheme 3) was computed as a non-pericyclic benchmark. The similarity between the magnetic behavior of the transition structures of **1b** $R_2 = O^-$ and model **3** confirms that they best represent pure anionic mechanisms.[9] The ACID representation (Fig. 2), albeit not conclusive, agrees with this picture, displaying at an isosurface density value of 0.030 a closed cyclic induced density for the counterion-bound allenolate, which indicates an aromaticity that is absent in the non-cyclic representation of the anionic transition structure.

The representations in Figs. 1 and 2 show that the effect of the lithium cation, so often dismissed as simply a counterion, is far from being negligible, specially for experiments carried out in THF, where a strong association of the lithium with the allenolate is expected. In this delicate balance of ionic–pericyclic contributions, it seems that the presence of the lithium cation and the concurrent decrease in the polarization of the reacting termini (the APT charge difference q_{C1}–q_{C5} changes from 0.90 and 0.81 for **1b tsE** and **1a tsZ** with $R_2 = O^-$, to 0.14 and 0.08 for **1b tsE** and **1a tsZ** with $R_2 = OLi$) tips the scale to the latter.

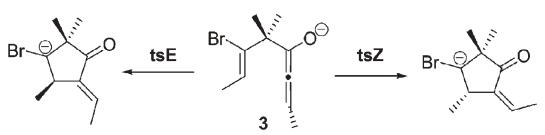

Scheme 3 Anionic cyclization of analog **3**, with a methyl group instead of the acetate (no further evolution of the bromo carbanion was studied). $\Delta\Delta G^{\ddagger}$ in this case is negligible (0.16 kcal mol^{-1}), and favors **tsE**.

To summarize, the remarkable stereospecificity of the cyclization of allenolate allyl carbamates **i** described by Hoppe *et al.* can be attributed to the geometric constraints needed for an effective charge donation from the π system of the allenolate ($\pi^*_{C4–O^-}$ or $\pi^*_{C4–C5}$, depending on the absence or the presence of a lithium cation) to the $\sigma^*_{C3–O9}$ orbital in concerted paths. In contrast, the alternate rotations occur through a stepwise mechanism. For the favored paths, analysis of the NICS values and ACID representations help establish the difference between the lithium-bound and the anionic systems, with transition states that are essentially pericyclic for the former and ionic for the latter. Depending upon the degree of ionic interaction ($O^-…Li^+$) in the putative intermediate allenolate **ii**, the stereospecific rearrangement of **i** into **iii** could show dominant features of pericyclic (torquoselective) or ionic processes, or a blend of both.

We thank the Ministerio de Educación y Ciencia (SAF04-07131) for financial support, and the CESGA for the allocation of computer resources. We are indebted to Prof. R. Herges for a copy of his ACID program.

Notes and references

1 C. Schultz-Fademrecht, M. A. Tius, S. Grimme, B. Wibbeling and D. Hoppe, *Angew. Chem., Int. Ed.*, 2002, **41**, 1532.
2 O. N. Faza, C. S. López, R. Álvarez and A. R. de Lera, *Chem.-Eur. J.*, 2004, **10**, 4324.
3 M. A. Tius, *Acc. Chem. Res.*, 2003, **36**, 284; H. Hu, D. Smith, R. E. Cramer and M. A. Tius, *J. Am. Chem. Soc.*, 1999, **121**, 9895.
4 IRC were only calculated for the (3*R*,5a*R*)-**4** transition structures, on the understanding that the results for the (3*S*,5a*R*)-**4** are equivalent.
5 O. N. Faza, C. S. López, R. Álvarez and A. R. de Lera, *Org. Lett.*, 2004, **6**, 905.
6 On most described examples of torquoselectivity, this rotational preference is determined by the substituents at the cyclization termini[2,5,7].
7 W. R. Dolbier, H. Koroniak, K. N. Houk and C. Sheu, *Acc. Chem. Res.*, 1996, **29**, 471; S. Niwayama, A. E. Kallel, C. Sheu and K. N. Houk, *J. Org. Chem.*, 1996, **61**, 2517.
8 R. Herges and D. J. Geuenich, *J. Phys. Chem. A*, 2001, **105**, 3214.
9 A scrutiny of this reaction is ongoing. The residual shieldings observed (low, but noticeable values in curves that maintain the characteristic shape of π^1 aromaticity), might be attributed to some kind of homoaromatic interaction, also present in other intramolecular S_N2' processes, as can be seen in Fig. 1.
10 All computations have been performed using DFT in Gaussian 03.[11] B3LYP with the 6-311G* basis set was used to compute the geometries, energies, and normal-mode vibration frequencies of the starting products and the corresponding transition structures. The stationary points were characterized by means of harmonic analysis. An analysis of the wavefunction stability was also carried out for all stationary points. In several significant cases intrinsic reaction coordinate (IRC) calculations were performed to unambiguously connect transition structures with reactants and products. The natural bond orbital (NBO) method was used to obtain secondary interactions between localized orbitals. For the study of the charge distribution, Cioslowski's APT puntual charges were used. Nucleus independent chemical shifts (NICS) were calculated by means of the gauge-independent atomic orbitals (GIAO) method along an axis perpendicular to the molecular plane. The ACID[8] method (based on the anisotropy of the current-induced density) was used to evaluate the electronic delocalization on aromatic transition structures.
11 M. J. Frisch, *et al.*, *Gaussian 03, Revision B.01*, Gaussian Inc., Pittsburgh PA, 2003.